Cold Regions Science and Technology 173 (2020) 103024

Contents lists available at ScienceDirect

Cold Regions Science and Technology

journal homepage: www.elsevier.com/locate/coldregions

Freeze-thaw cycling impact on the shear behavior of frozen soil-concrete interface

Pengfei He[a,b,e], Yanhu Mu[b], Zhaohui Yang (Joey)[c,*], Wei Ma[b,e], Jianhua Dong[d], Yongting Huang[b,e]

[a] School of Science, Lanzhou University of Technology, Lanzhou 730050, China
[b] State Key Laboratory of Frozen Soil Engineering, Northwest Institute of Eco-Environment and Resources, Chinese Academy of Sciences, Lanzhou 730000, China
[c] College of Engineering, University of Alaska Anchorage, Anchorage, AK 99508, USA
[d] School of Civil Engineering, Lanzhou University of Technology, Lanzhou 730050, China
[e] University of Chinese Academy of Science, Beijing 100049, China

ARTICLE INFO

Keywords:
Freeze-thaw
Frozen soil-concrete interface
Peak and residual displacement
Shear strength parameters
Direct shear test

ABSTRACT

The shear behavior of a frozen soil-structure interface plays a vital role in analyzing the performance of engineered structures in cold regions. This study investigates the freeze-thaw cycling impact on the shear behavior of a frozen soil-concrete interface by direct shear tests. Test specimens consisting of a Portland cement concrete disk and frozen loess with an initial moisture content ranging between 9.2% and 20.8% were prepared and conditioned at various sub-zero temperatures (i.e., −1 °C, −3 °C, and − 5 °C) and freeze-thaw (F-T) cycles (i.e., 0, 5, 10, and 20). Experimental results, including shear stress - horizontal displacement curves, the displacements and shear strengths at both peak and residual status, are presented and analyzed. In particular, the influence of F-T cycling on shear behavior is examined. The peak displacement is found to increase linearly with increasing initial moisture content, but their correlation weakens as the number of F-T cycling increases. However, the residual displacement is found to be insensitive to the initial moisture content, temperature, normal stress, and F-T cycling. While the residual friction angle is slightly larger than the peak one before F-T cycling, both gradually increase with an increasing number of F-T cycling. Large cohesion in the peak strength, especially at lower temperatures, completely diminishes in the residual strength due to damage of ice bondage, resulting in a significant shear strength loss between the peak and residual status. The impact of F-T cycling on the interface shear behavior can be attributed to moisture migration toward, formation and accumulation of ice films at the interface. The findings from this study including the shear strength parameters and the displacements at both peak and residual status, can be used to simulate the performance of engineered geotechnical assets such as pile foundations, retaining walls, and earth dams or irrigation channels with concrete linings in cold regions.

1. Introduction

The shear behavior of a frozen soil-structure interface is of great importance in analyzing the performance of engineered geotechnical assets, such as pile foundations, retaining walls, canal works and box culverts that involve soil-structure interaction, in the broad cold regions, as many failures have been attributed to seasonal ground freezing (Bondarenko and Sadovskii, 1975; Volokhov, 2003; Weaver and Morgenstern, 1981; Wen et al., 2016). Fig. 1a illustrates the frozen soil surrounding a reinforced-concrete gravity retaining wall in the winter season and the shear forces acting at the frozen soil-concrete interface (Lai et al., 2002; Rui et al., 2016; Zhu and Michalowski, 2013). The frost heave generally occurs in the direction of heat flux, resulting in shear and normal stress on the back of the retaining wall and the shear resistance at the base of the wall. These stresses can cause excessive deformation, stress, or even structural failure. For example, a number of precast concrete panels of a Mechanically Stabilized Earth wall in the western United States collapsed in early spring 2007, due to relative displacement or slip between the soil and the wall caused by frost heave (Neely, 2010). The behavior of the interfaces between the retaining wall base and the foundation soil and between the fill material and retaining wall plays pivotal roles in the performance of retaining walls in the winter season. Fig. 1b depicts the winter season loading conditions of concrete surface linings commonly used as a seepage barrier on earth- or rock-fill embankments, dams, or waterway, or in highway drainage channels. The concrete lining is under the combined

* Corresponding author.
E-mail address: zyang2@alaska.edu (Z. Yang).

https://doi.org/10.1016/j.coldregions.2020.103024
Received 2 November 2019; Received in revised form 18 January 2020; Accepted 26 February 2020
Available online 27 February 2020

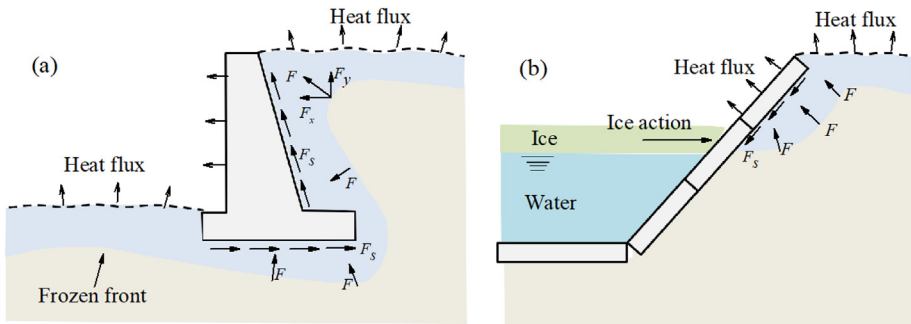

Fig. 1. Engineering examples involving the interaction at frozen soil-concrete interfaces: (a) retaining walls, and (b) concrete linings of an earth dam or drainage channel in cold regions. *F* is the frost heave force, and *Fs* is the shear force at the interfaces.

loading of ice pushing, frost heave force, and shear resistance afforded by the soil-concrete lining interface (Qing et al., 2011; Wei, 2007; Woo et al., 2009) and is susceptible to damage. Severe and wide-spread damage was reported to occur in concrete linings of dams near the water level (Sun et al., 1998; Qing et al., 2011) and railway embankment drainage trench (Tian et al., 2019), and in other hydraulic structures (e.g., Hirayama, 1976; Sadzevicius et al., 2013). The shear strength of the soil-structure interface is also a crucial factor for assessing the bearing capacity and long-term stability of infrastructure embedded in the frozen ground (Aldaeef and Rayhani, 2018; Bondarenko and Sadovskii, 1975; Parameswaran, 1978; Wen et al., 2016).

Many researchers have studied the shear behavior of the soil-structure interface via field tests (Penner and Irwin, 1969; Johnston and Ladanyi, 1972; Parameswaran, 1978; Biggar and Sego, 1993a, 1993b; Feng et al., 2016), laboratory experiments (Andersland and Alwahhab, 1982; Liu et al., 2014a, 2014b; Wen et al., 2016; Aldaeef and Rayhani, 2017, 2018), and theoretical or numerical analyses (Foriero and Ladanyi, 1995; Liu and Ling, 2008; Liu et al., 2014a, 2014b). In particular, Liu et al. (2014a, 2014b) studied the shear behavior of frozen soil-concrete interfaces by a large-scale direct shear test system at subzero temperatures and their results show that temperature and moisture content have a significant effect on the peak shear strength, but have little impact on the residual shear strength. Several studies (Shi et al., 2018; Wang et al., 2019; Zhao et al., 2014) focused on the interface behavior of artificial frozen soil-steel interface commonly encountered during shield tunneling by Tunnel Boring Machine and found that temperature and surface roughness have significant impact on the interface shear behavior including both the peak and residual shear strengths. Wen et al. (2016) investigated the adfreeze strength of frozen soil-fiberglass reinforced plastic interface by direct shear tests and concluded that the cohesion is controlled by temperature and moisture content and the friction angle is, however, only affected by moisture content. Lv and Liu (2015) and Zhao et al. (2014) studied the dynamic shear properties of the interface between frozen soil and concrete or steel and found that the peak shear stress decreases quickly at the beginning and then gradually stabilizes with an increasing number of cyclic shearing. These studies show that the shear strength depends mainly on the strengths of the interface materials, including the soil and the counteracting materials, initial water or ice content of frozen soil, temperature, normal stress, loading rate, among others.

Freeze-thaw (F-T) cycling in seasonally frozen soil or the active layer of permafrost not only affects soil mechanical properties but also the shear behavior at the frozen soil-structure interface and its impact should be accounted for in cold regions engineering (Qi et al., 2008; Choi et al., 2014). Many researchers have reported that F-T cycling can significantly alter soil physical properties including particle size distribution, Atterberg limits, dry density, and permeability, and mechanical properties (Viklander and Eigenbrod, 2000; Shen, 2004; Qi et al., 2008; Gutierrez et al., 2008; Li et al., 2012). More specifically, Viklander (1998) noted that F-T cycling could lead to the densification of loose soils and loosening of dense soils. Zhang et al. (2016) pointed out that F-T cycling can induce fragmentation of coarse particles and aggregation of fine particles, and the particle size tends to become homogeneous. Liu et al. (2016) showed that F-T cycling has a significant influence on the mechanical properties of silty sand and found that the elastic modulus and strength can decrease by up to 45% after 12 cycles. Li et al. (2018) studied the influence of F-T cycling on loess and found that the unconfined compressive strength, elastic modulus, and cohesion decrease with increasing F-T cycles, whereas the axial compression strain increases. Additionally, F-T cycling was found to induce complex moisture migration in porous materials, including soils and concrete (Shoop and Bigl, 1997; Škerget et al., 2018), therefore altering the moisture distribution at a soil-structure interface. These actions associated with F-T cycling, as pointed out by previous studies, can lead to changes in soil particle re-arrangement, moisture re-distribution, and contact conditions, which in turn can induce a significant impact on the shear behavior of soil-structure interfaces.

In summary, most existing studies focused on the shear strength of a frozen soil-structure interface or the F-T cycling impact on the mechanical properties of soils. The shear displacement at which the peak strength occurs and the impact of F-T cycling on the shear behavior of a frozen soil-structure interface was largely ignored. This paper aims to investigate the shear behavior of a frozen soil-concrete interface, including both shear strength and displacement characteristics and the impact of F-T cycling on the interface shear behavior. Factors considered include temperature, initial moisture content, normal stress, and the number of F-T cycling. Results including the shear stress-horizontal displacement relationship, peak and residual shear strengths, and displacements of the interface are presented and analyzed.

2. Experimental procedure

A direct shear apparatus was used to collect experimental data on the shear behavior of frozen soil-concrete interfaces. This section describes the test soil and concrete, interface specimen preparation procedure, F-T cycling, and testing procedure.

2.1. Test soil and concrete

The soil used in this study was sampled from a shallow surface layer of loess in Gansu Province, China. The soil was naturally dried, crushed by a roller, and then passed through a sieve of 2-mm openings. The soil has the following index properties: specific gravity $G_s = 2.70$, liquid limit $LL = 26.3\%$, plastic limit $PL = 18.2\%$, plasticity index $PI = 8.1\%$, the maximum dry density $\rho_{d\text{-}max} = 1.912\ \mathrm{g/cm^3}$, and the optimum moisture content $\omega_{opt} = 13.0\%$. Fig. 2 shows the grain-size distribution obtained by the laser diffraction method (The standard ISO 13320-1:1999). The soil was classified as sandy lean clay (CL) according to the unified soil classification system. The internal friction angle of soil with

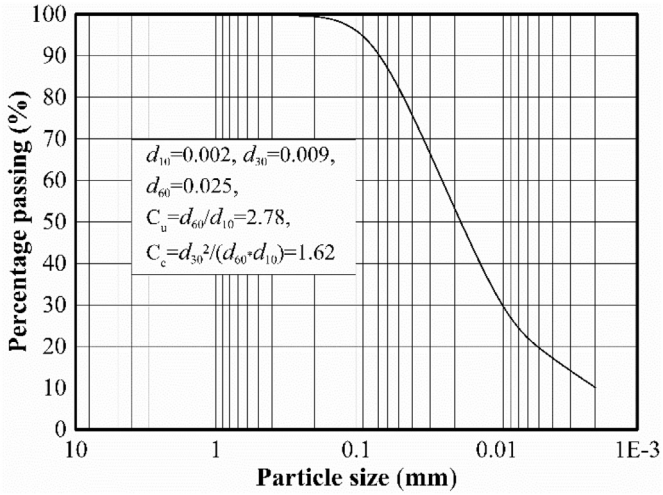

Fig. 2. Grain-size distribution of the test soil.

a dry density of 1.68 g/cm^3 at the optimum moisture content was found to be 29.0° (Li et al., 2018). For preparing test soils, distilled water was added to dry soil to achieve a certain target initial moisture content by weight. The soil sample was then fully mixed, sealed, and stored for 12 h at 20 °C to ensure uniform moisture distribution. Since the natural moisture content of soil generally varies from 10%–20%, four initial moisture contents (w_i), i.e., 9.2%, 13.1%, 17.1%, and 20.8%, corresponding to the degree of saturation (S_r) of 36.7%, 52.3%, 68.2%, and 83.0%, respectively, was chosen to investigate its effects on the shear behavior of the soil-concrete interface. It is worth noting that there is 0.8% salt (primarily sodium chloride) in the soil, and the initial freezing point decreases from − 0.98 °C to − 2.88 °C when the initial water content decreases from 21% to 9% (Wu et al., 2019).

Concrete disks with 20 mm in height and 61.8 mm in diameter were made from mortar consisting of ordinary Portland cement (Grade 32.5), natural river sand, and water by a mix ratio of 1.8:3:1. All samples were cured for 28 days after pouring (GBJ-82-85, 1997). Particles larger than 4.75 mm were removed from the river sand to minimize size effects and maintain consistent surface roughness. Note that the height of the concrete disks was precisely controlled to 20 mm for the induced shear failure plane to be aligned with the soil-concrete interface in a direct shear box.

2.2. Soil-concrete specimen preparation

Containers with a height of 40 mm and an inner diameter of 61.8 mm were used to prepare soil-concrete specimens as follows. A thin layer of Vaseline was applied on the container internal surface to provide lubrication and allow easy specimen extrusion. A concrete disk was then slid into a container, as shown in Fig. 3a. The prepared soil was subsequently placed on top of the concrete disk and compacted to a target dry density of 1.68 g/cm^3 and a height of 20 mm. The soil-concrete specimen, together with the container, was immediately sealed with plastic film after preparation and stored in an environmental chamber for 24 h to allow quick freezing at −20 °C. No significant change in height was observed after freezing. The specimens were then extruded by a hydraulic jack. No concrete spalling or damage to frozen soil was observed after extrusion, as exemplified in Fig. 3b. Before shear testing, all specimens were conditioned to selected test temperatures for 12 h. Three test temperatures, i.e., −1 °C, −3 °C and − 5 °C, were considered. A previous study (He et al., 2018) found that the average peak friction angle at the soil-concrete interface at 20 °C was 28°.

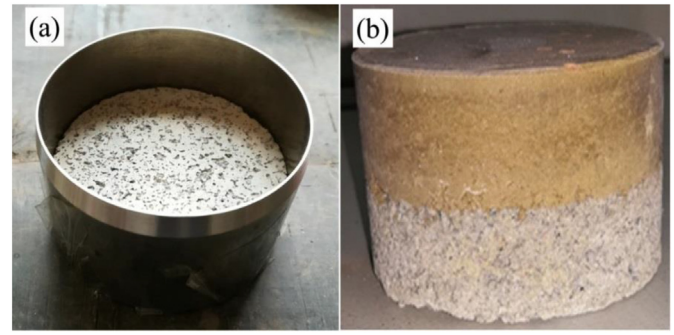

Fig. 3. Specimen preparation: (a) a container with a concrete disk placed in the container, and (b) a typical soil-concrete specimen after extrusion.

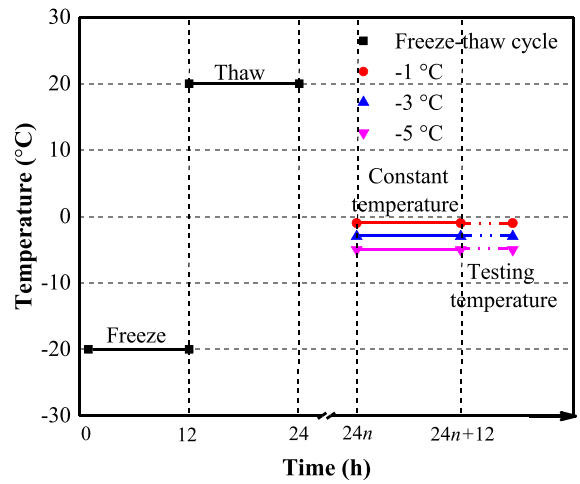

Fig. 4. Thermal paths during F-T cycling and conditioning. n is the number of F-T cycles.

2.3. Freeze-thaw cycling

During the F-T cycling of the specimens, the temperature varied between −20 °C and 20 °C based on the observed temperatures in the study site, as illustrated in Fig. 4. In a signal F-T cycle, the specimens were subjected to freezing in an environmental chamber with the temperature set at −20 °C for a period of 12 h and then thawed at 20 °C for 12 h. This procedure was repeated for selected number of cycles, i.e., 0, 5, 10, or 20. After F-T cycling, specimens were placed in an environmental chamber set at a certain test temperature for 12 h to allow thermal equilibrium. Three test temperatures, i.e., −1 °C, −3 °C, and − 5 °C, were selected to investigate the temperature effects.

2.4. Testing procedure

All tests were carried out by using a four-unit joint direct shear apparatus by displacement control, as illustrated in Fig. 5. A constant shear displacement rate of 0.8 mm/min was applied to the lower half of the shear boxes during testing. It is noted that the shear displacement was applied to the four units simultaneously, and the shear force was measured at each unit. Due to equipment limitations, the vertical displacement during shearing was not measured. The normal stress applied to the soil-concrete interface (σ_N) was 50 kPa, 100 kPa, 200 kPa, or 300 kPa. During testing, the apparatus was placed in a cold room with its temperature-controlled to within ± 0.5 °C of the test temperature. The containers with the specimens installed were covered by insulation material and installed quickly to the direct shear apparatus to minimize the disturbance to the specimen temperature. As the direct shear test can be conducted within 10 min, the fluctuation of

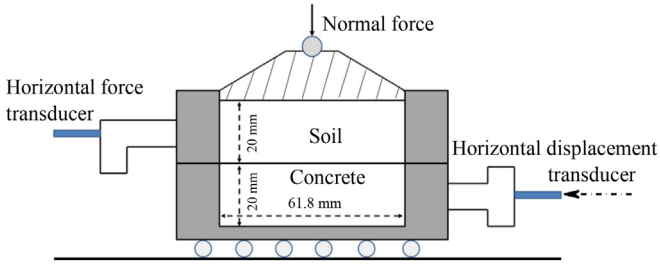

Fig. 5. Illustration of the direct shear apparatus with a soil-concrete specimen installed.

temperature in the cold room was believed to have very limited, if any, influence on the specimen temperature. In summary, there are a total of 192 cases, considering all possible combinations of the four testing parameters, including w_i (9.2%, 13.1%, 17.1%, and 20.8%), T (−1 °C, −3 °C, and − 5 °C), F-T number (0, 5, 10, and 20), and normal stress σ_N (50 kPa, 100 kPa, 200 kPa, and 300 kPa).

3. Experimental results

3.1. Shear stress vs. displacement

In general, the shear stress - horizontal displacement curves from this study exhibited a strain-softening behavior, as also observed in other studies (Liu et al., 2014a, 2014b; Shi et al., 2018; Ji et al., 2019). Fig. 6 illustrates a typical shear stress τ vs. shear displacement δ curve, which can be divided into three stages: pre-peak, post-peak, and residual. At the pre-peak stage, the shear stress increases with increasing displacement until it reaches a maximum value. The maximum shear stress is defined as the peak shear strength, τ_p, and the displacement at which τ_p occurs is defined as the peak displacement, δ_p. Within this stage, the ice crystal is intact at the initial linear portion, followed by a curvilinear portion when the ice crystal is ruptured, and the resistance is mobilized (Biggar and Sego, 1993a, 1993b). Toward the end of this stage, the contribution from ice crystals to the shear resistance reaches a maximum, helping achieve a peak in the shear stress-displacement curve. In the post-peak stage, a significant reduction occurs in the shear stress due to quickly decreasing adhesion as the ice bondage at the interface begins to break with increasing displacement (Peretrukhin et al., 1978). The shear stress stabilizes as the displacement increases and eventually remains unchanged in the residual state. The shear stress that remains constant with increasing displacement is defined as

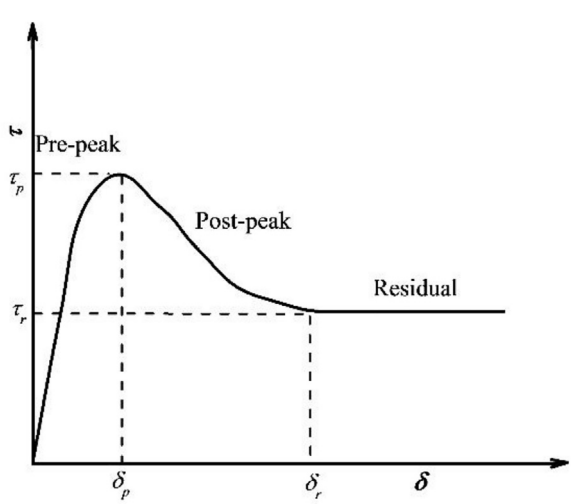

Fig. 6. Typical shape of a shear stress – horizontal displacement curve of a frozen soil-structure interface.

the residual strength (τ_r), and the displacement corresponding to the first occurrence of τ_r is defined as the residual displacement, δ_r.

Figs. 7 through 9 display selected shear stress vs. horizontal displacement curves to illustrate the impact of F-T cycling, temperature, initial moisture content, and normal stress. Note that the device tended to have issues with the control system when the shear stress experienced a peak value but recovered when the shear stress stabilized. This issue resulted in a gap in the data in the post-peak stage but did not affect the analyses as it was still possible to reliably identify the peak and residual shear stress as well as the corresponding displacements for all cases. Fig. 7 compares the interface shear behavior for different numbers of F-T cycling and temperatures at $w_i = 13.1\%$ and $\sigma_N = 200$ kPa. It is seen from Fig. 7 that F-T cycling had some impact on the peak and residual stresses and corresponding displacements, although no clear trend can be observed. For instance, τ_p increases with an increasing number of F-T cycling at −1 °C as shown in Fig. 7a. The same cannot be observed in Fig. 7b and c for −3 °C or − 5 °C. Comparing Fig. 7a, b and c, it is clear that the temperature had a significant impact on the peak shear strength but small or no impact on the residual strength, and its effect on the corresponding displacements is not prominent. Specifically, τ_p increases consistently with decreasing temperature under said moisture and normal stress conditions.

Fig. 8 compares the shear behavior at $T = -5$ °C and $\sigma_N = 100$ kPa for different initial moisture contents. It is seen that the initial moisture content had a consistent influence on the peak shear strength and moderate impact on the corresponding displacement but little on the residual strength and displacement. The peak shear strength and displacement tend to increase as the initial moisture content increases. Fig. 9 compares the shear behavior at $T = -1$ °C and $w_i = 9.2\%$ for different normal stresses. At a given number of F-T cycling, the peak and residual shear stresses generally increased with increasing normal stress. However, the impact of normal stress on the peak and residual displacements is not significant. It is interesting to observe that, while most of the stress-displacement curves exhibit a strain-softening behavior, the curve for $\sigma_N = 300$ kPa and 20 F-T cycles in Fig. 9c displays a strain-hardening behavior, likely due to suppression to the dilatancy at higher normal stress.

3.2. Peak and residual displacements

As mentioned previously, little attention has been paid to the displacements, which are as important as the strengths for describing the shear behavior of a frozen soil-structure interface (Andersland and Alwahhab, 1982). Figs. 10 and 11 respectively describe the variation of the peak and residual displacements with various factors, including the initial moisture content, F-T cycling, temperature, and normal stress. It is noted that the residual displacement was selected where the shear stress remained constant or experienced little change with increasing displacement (Fig. 6). It is apparent from Fig. 10 that the peak displacement almost increased linearly with increasing initial moisture content (Fig. 10a), but was insensitive to F-T cycling (Fig. 10b), temperature (Fig. 10c), and normal stress (Fig. 10d). The residual displacement shown in Fig. 11, however, seems insensitive to all of these four factors.

It would be worthwhile to examine how the trend between the peak displacement and initial moisture content varies with F-T cycling. Fig. 12 shows the peak displacement vs. initial moisture content at an increasing number of F-T cycling. Also displayed in Fig. 12 is a linear relationship, $\delta_p = a + b\,w_i$, obtained by the best fitting. Table 1 lists the parameters a and b of the linear relationship, the coefficient of determination, R^2, and the standard deviation, SD. It is seen from Fig. 12 and Table 1 that, while the linear trend holds for specimens subjected to 0, 5, and 10 F-T cycles, the slope of the linear relationship, i.e., b, showed a decreasing trend and the scattering in the data increased, as evidenced by the decreasing value of R^2 and increasing value of SD. After 20 F-T cycles, the value of R^2 became so small that the peak

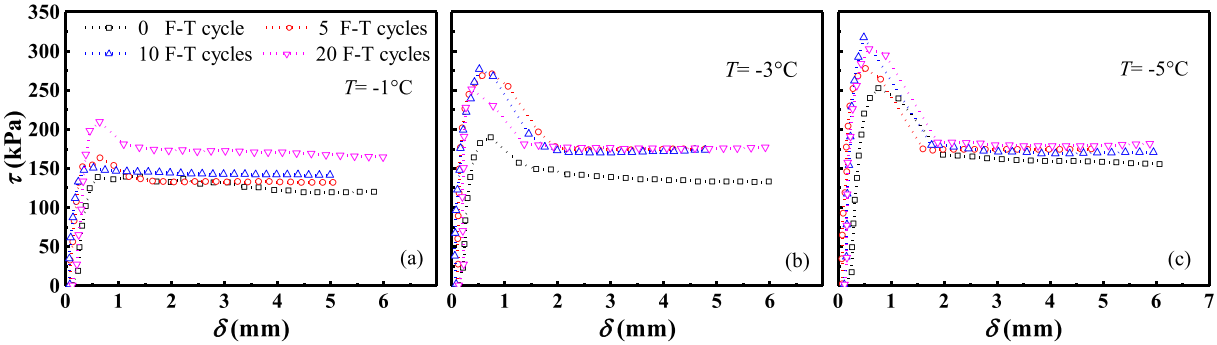

Fig. 7. Comparison of the interface shear behavior at w_i = 13.1% and σ_N = 200 kPa for different F-T cycles and temperatures: a) –1 °C, b) –3 °C, and c) –5 °C.

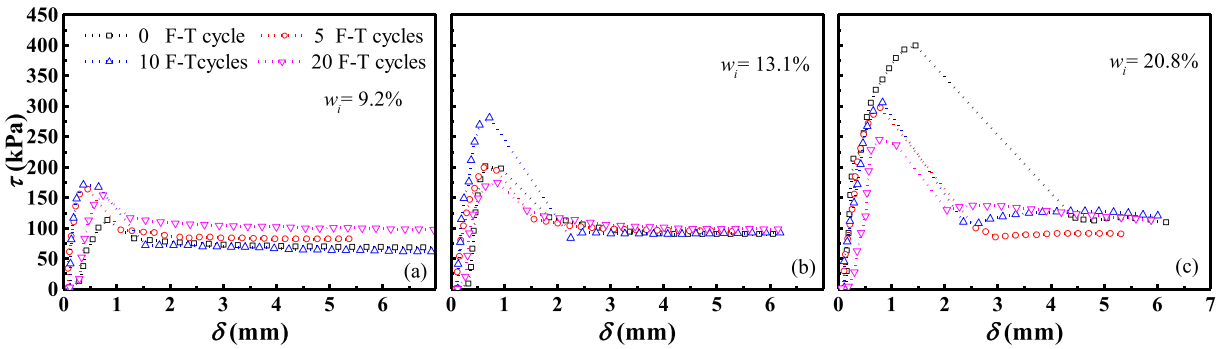

Fig. 8. Comparison of the interface shear behavior at $T = -5$ °C and σ_N = 100 kPa for increasing initial moisture content: a) w_i = 9.2%, b) w_i = 13.1%, and c) w_i = 20.8%.

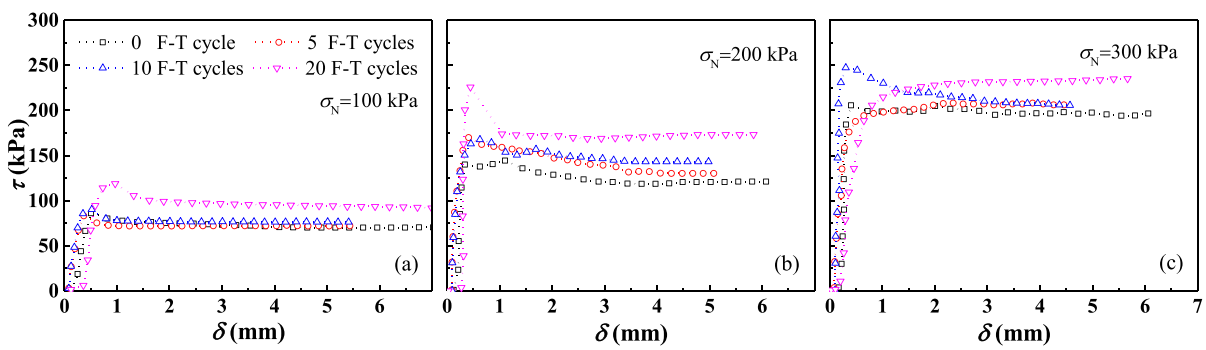

Fig. 9. Comparison of interface the shear behavior at $T = -1$ °C and w_i = 9.2% for increasing normal pressure: a) σ_N = 100 kPa, b) σ_N = 200 kPa, and c) σ_N = 300 kPa.

displacement can be deemed as independent of the initial moisture content. This phenomenon was likely the result of moisture migration toward the interface during F-T cycling, which will be revisited in the Discussions section. The arithmetic mean (AM) of the peak displacement was found to be 0.8 mm, and the SD was 0.4 mm, which can be used to describe the peak displacement of the interface.

As the residual displacement was shown to be insensitive to any of the four test variables, all data points were displayed against the initial moisture content in Fig. 13 for ease of visualization. It was found that the residual displacement varied between 1 mm and 5 mm with a mean of 3.3 mm and an SD of 1.0 mm. The residual strength was chosen as the shear stress corresponding to the upper end of residual displacements, i.e., 5 mm, for all specimens.

3.3. Peak and residual strengths

There is no doubt that the peak shear strength is a crucial parameter as it describes the maximum shear resistance at a soil-structure interface. Fig. 14 describes typical variations of τ_p vs. F-T cycles for all w_i, T under selected σ_N. Note that the data corresponding to 20 F-T cycles for w_i = 9.2% and $T = -5$ °C under σ_N = 300 kPa was not available, but it did not affect the observation of the overall trend. It is seen from Fig. 14 a and b that, for the same w_i and σ_N, the value of τ_p overall increased with decreasing temperature, which is expected as more pore water freezes at the interface at a lower sub-freezing temperature and the shear strength of ice also increases with decreasing temperature (Liu et al., 2014a, 2014b; Zhao et al., 2014; Wen et al., 2016; He et al., 2018). One can also see that, as the number of F-T cycling increased, the value of τ_p remained almost constant under σ_N = 50 kPa and increased slightly under σ_N = 300 kPa for both $T = -1$ °C and -3 °C. At $T = -5$ °C, however, both F-T cycling and w_i had a significant impact on τ_p. Specifically, τ_p increased from 64.8 kPa to 160.0 kPa after 20 F-T cycles for specimens with w_i = 9.2%. At higher values of w_i, i.e., 13.1%, 17.1%, and 20.8%, τ_p demonstrated a decreasing trend with F-T cycles, which is especially evident for low σ_N value (e.g., 50 kPa, Fig. 14a). At a higher σ_N (e.g., 300 kPa, Fig. 14b),

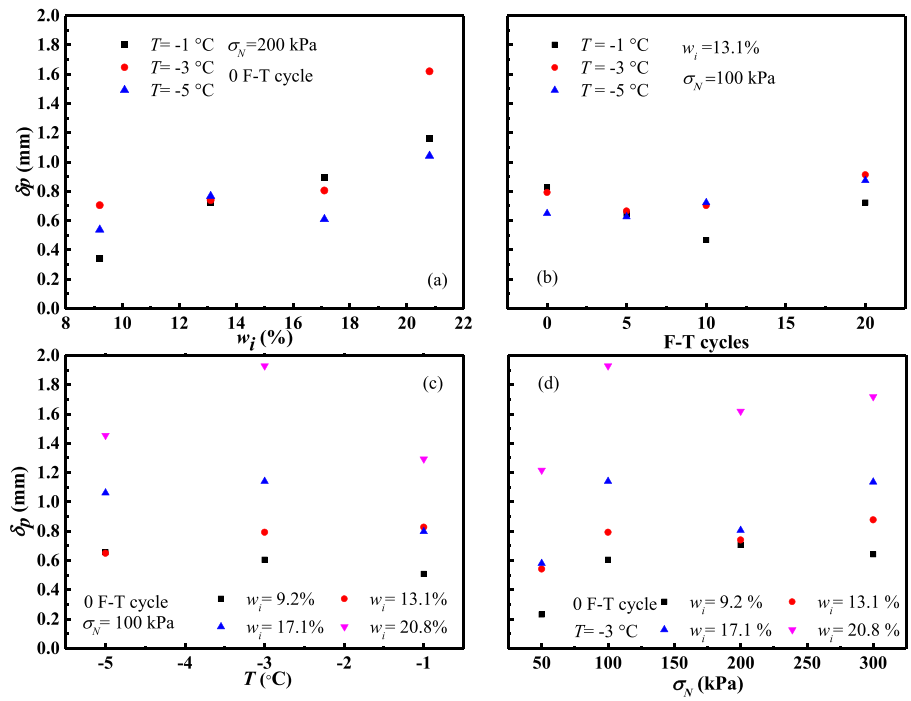

Fig. 10. Variation of the peak displacement with a) moisture content, b) F-T cycling, c) temperature, and d) normal stress.

this trend is still visible but somewhat suppressed. Comparing Fig. 14a with b, one can observe that, for the same w_i and T, τ_p increased substantially with the increase of σ_N, implying a significant contribution of friction to the interface resistance.

Since friction was evidenced to play a big role in the interface shear behavior, the Mohr-Coulomb shear failure criterion was adopted to analyze the peak shear strength further:

$$\tau_p = c_p + \sigma_N \tan(\phi_p) \tag{1}$$

where c_p is the peak interface cohesion, and ϕ_p the peak interface friction angle. Fig. 15 shows the variation of c_p vs. F-T cycles for all w_i and T. c_p generally increased with decreasing temperature, which is similar to the overall trend of τ_p vs. F-T cycles for various T as presented in Fig. 14, indicating an important contribution of ice adhesion to the peak interface shear resistance. As shown in Fig. 15a, the minimum and maximum values of c_p at -1 °C were respectively 7.6 kPa and 42.8 kPa, confirming that no significant ice bondage formed in the interface. It is seen from Fig. 15b that the minimum and maximum values of c_p at

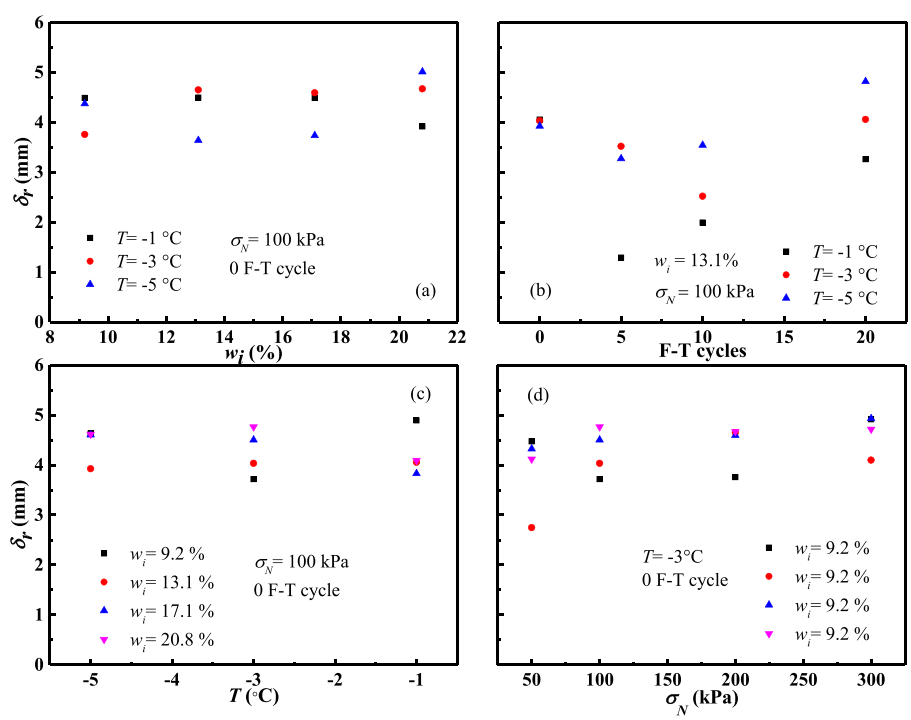

Fig. 11. Variation of the residual displacement with a) moisture content, b) F-T cycling, c) temperature, and d) normal stress.

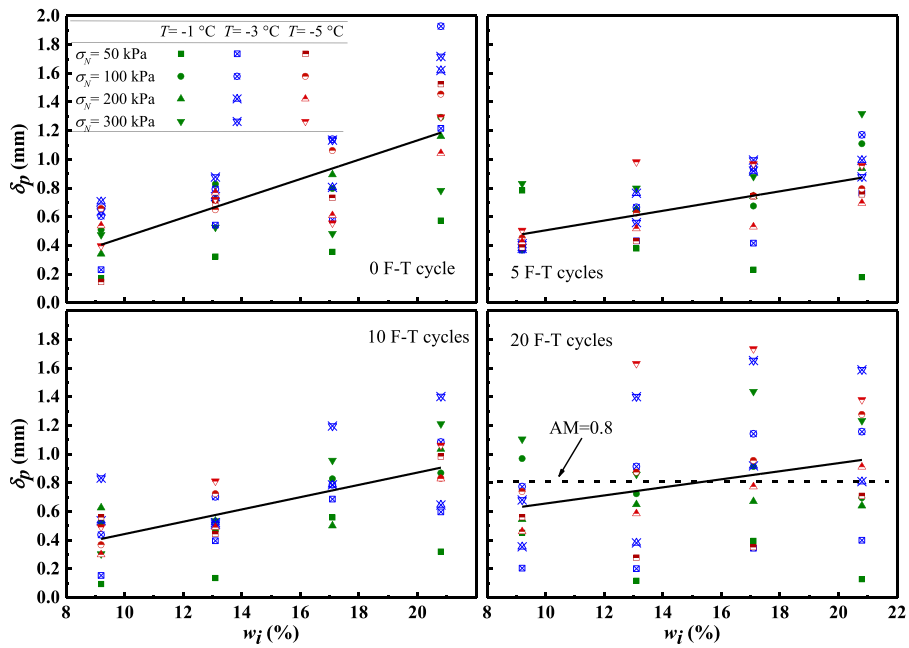

Fig. 12. Peak displacement vs. moisture content for an increasing number of F-T cycles.

Table 1
Parameters of the linear relationship between the peak displacement and initial moisture content.

Number of F-T cycling	a	b	R^2	Standard deviation
0	−0.215	0.067	0.523	0.279
5	0.166	0.034	0.312	0.216
10	0.014	0.043	0.419	0.225
20	0.374	0.028	0.061	0.414

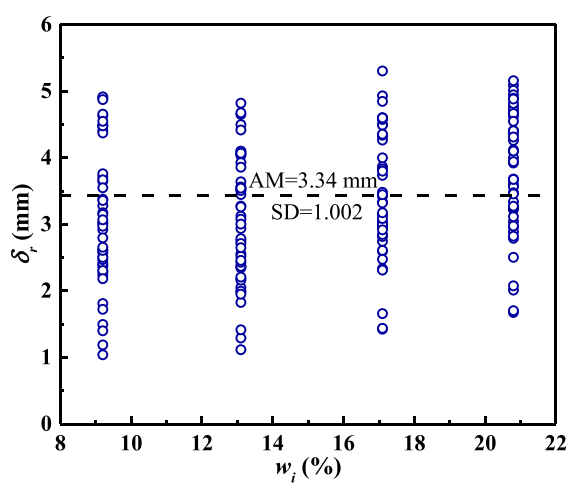

Fig. 13. The residual displacement vs. initial moisture content for all specimens.

$T = -3$ °C were respectively 38.2 kPa and 121.9 kPa, which are significantly larger than those at −1 °C and indicates that ice adhesion starts to make a significant contribution to τ_p. It is also clear from Fig. 15b that c_p is generally larger for higher initial water content since more pore water was frozen due to a higher initial freezing point (refer to Section. 2.1). It is worth noting that, at both −1 °C and − 3 °C, F-T cycling only slightly affected c_p for all w_i. At −5 °C, however, it is obvious from Fig. 15c that c_p increased significantly when compared with those at higher test temperatures, and F-T cycling had a noticeable impact. Overall, c_p increased with the increase of the moisture content at the same number of F-T cycles, primarily due to more ice bondage formed in the interface. It is interesting to observe that, with an increasing number of F-T cycling, c_p corresponding to $w_i = 9.2\%$ increases, whereas c_p for $w_i = 20.8\%$, 17.1%, and 13.1% decreases quite substantially. Specifically, the values of c_p corresponding to $w_i = 20.8\%$, 17.1%, and 13.1% decreased respectively from 315.6 kPa, 199.2 kPa, and 145.2 kPa to 226.4 kPa, 97.0 kPa, and 66.8 kPa after 20 F-T cycles.

Fig. 16 shows the values of ϕ_p vs. F-T cycles. One can see that, for all available T and w_i, ϕ_p increased with increasing F-T cycles. However, it appears that ϕ_p is not dependent on w_i and T. Hence, the average values of ϕ_p for all w_i and T at a various number of F-T cycles were computed and shown in Fig. 16 as well. The average ϕ_p increased from 30.1° to 39.2° after 20 F-T cycles, or an increase of about 9°. Fig. 16 also shows that the rise in the average ϕ_p was minimal when the number of F-T cycling increased from 10 to 20, indicating a stabilized peak frictional angle is achieved.

Fig. 17a and b illustrate the variation of τ_r vs. F-T cycles at all w_i and T under $\sigma_N = 50$ kPa and 300 kPa, respectively. Comparing Fig. 17 with Fig. 14, one can observe that the values of τ_r were much smaller than τ_p, especially for $\sigma_N = 50$ kPa. Overall, can see that the variation of τ_r with w_i and T was small and the impact of F-T cycling on τ_r was much less prominent than on τ_p, though a gradually increasing trend can be observed in τ_r for $\sigma_N = 300$ kPa. Nonetheless, comparing Fig. 17 a with b, one can see that the influence of σ_N on τ_r is much more pronounced than that on τ_p. Similarly, the results were analyzed by the Mohr-Coulomb shear failure criterion:

$$\tau_r = c_r + \sigma_N \tan(\phi_r) \tag{2}$$

where c_r is the residual cohesion, and ϕ_r is the residual friction angle. c_r was found to be negligible, which confirms that τ_r arises mainly from frictional resistance at the interface, as previously reported by Nidowicz and Shur (1998), Liu et al. (2014a, 2014b), and Lv and Liu (2015). Fig. 18 a, b, and c depicts the variation of ϕ_r with F-T cycles for all w_i at $T = -1$ °C, −3 °C and − 5 °C, respectively. The results again show that w_i and T had little effects on ϕ_r, whereas F-T cycling increased ϕ_r. One can observe that less scattering exists in the variation of ϕ_r with w_i than in that of ϕ_p. Therefore, the average values of ϕ_r for all w_i and test

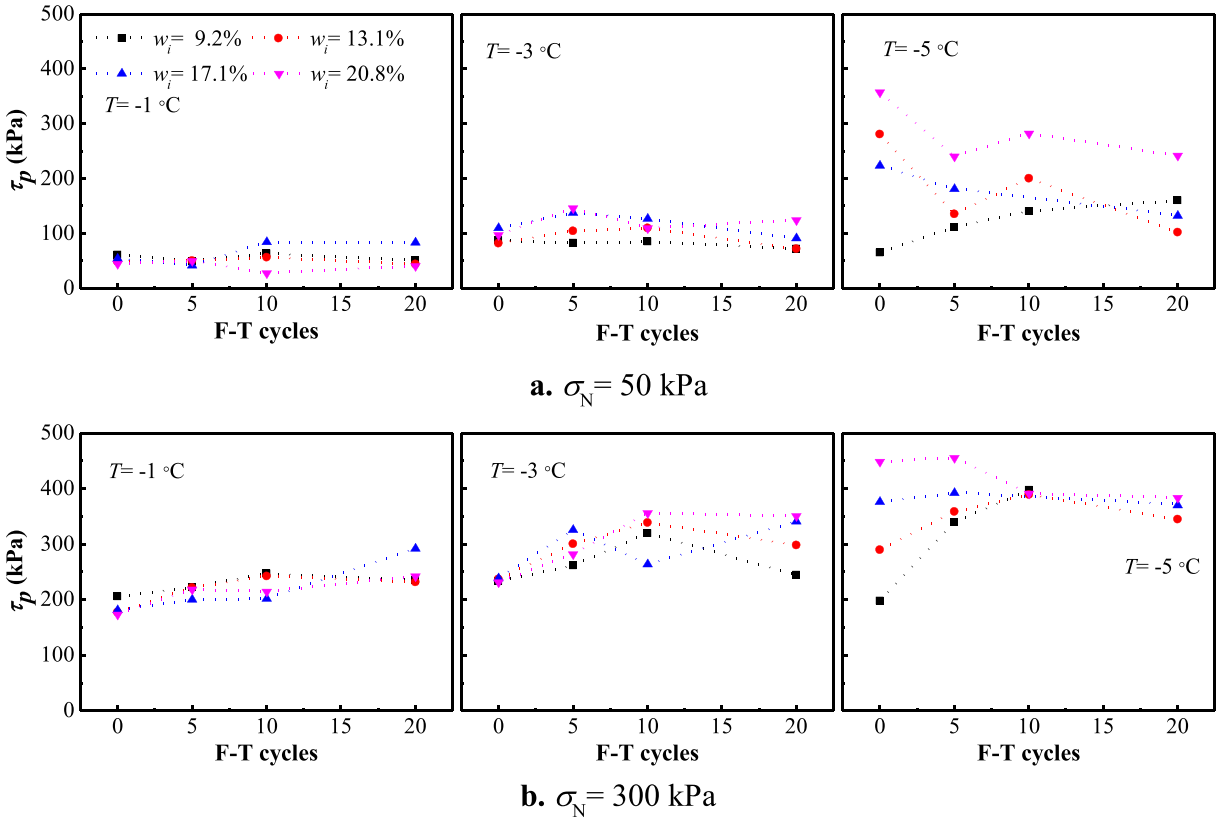

Fig. 14. Typical variations of the peak shear strength with F-T cycles at all initial moisture contents, test temperatures, and selected normal stress: a) σ_N = 50 kPa, and b) σ_N = 300 kPa.

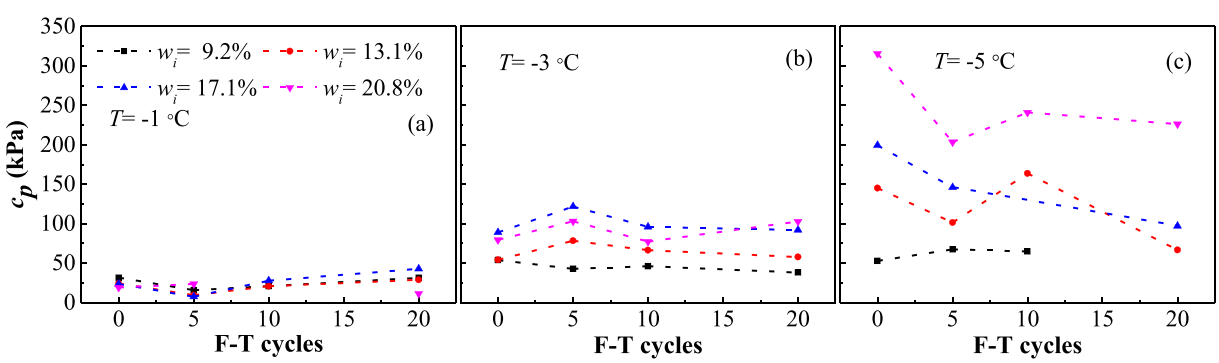

Fig. 15. Variation of the peak cohesion with F-T cycles for all initial moisture contents and test temperatures: a) $T = -1$ °C, b) $T = -3$ °C, and c) $T = -5$ °C.

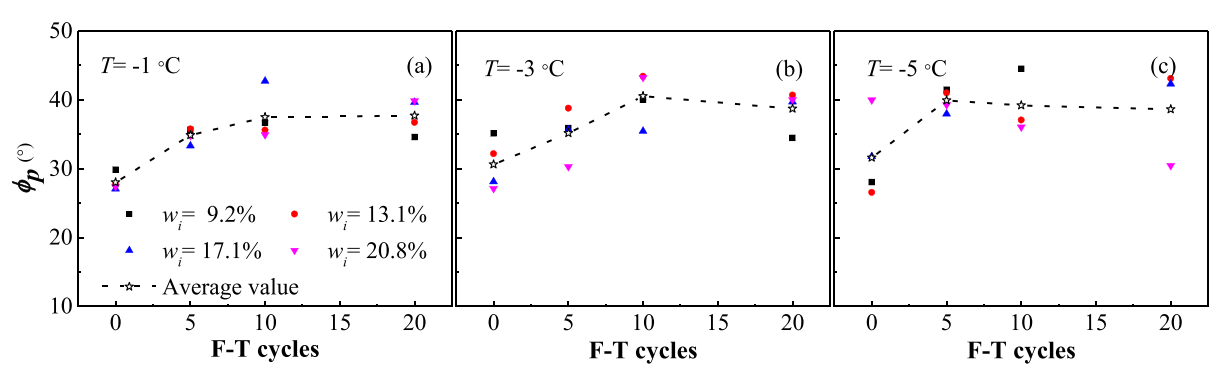

Fig. 16. Variation of the peak friction angle with F-T cycles for different initial moisture contents and test temperatures: (a) $T = -1$ °C, (b) $T = -3$ °C, and (c) $T = -5$ °C.

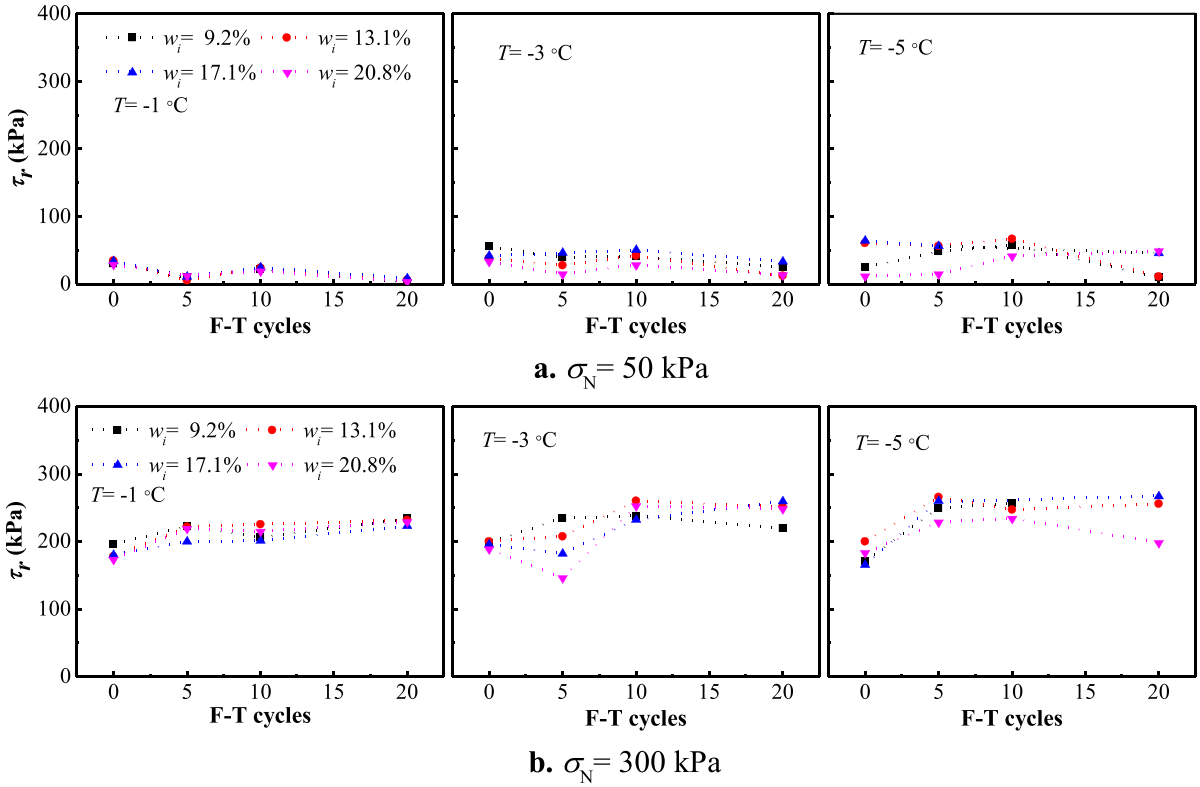

Fig. 17. Typical variations of the residual shear strength with F-T cycles for different initial moisture contents and test temperatures under a) σ_N = 50 kPa and b) σ_N = 300 kPa.

temperatures at various F-T cycles were computed and depicted in Fig. 18. The average ϕ_r increased from 33.5° to 39.6° after 20 F-T cycles, or an increase of about 6°. Again, the plots of the average ϕ_r vs. F-T cycles demonstrate a leveling trend at 10–20 F-T cycles, implying that a stabilized residual frictional angle is reached.

4. Discussions

4.1. General observations on shear strength parameters

Experimental results show that, before F-T cycling, the average ϕ_r, i.e., 33.5°, was slightly larger than the average ϕ_p, i.e., 30.1°. This observation is consistent with previous studies (e.g., Sadovskiy, 1973). After 20 F-T cycles, the average ϕ_p and ϕ_r increased to the same value, i.e., 39°. That is to say that no significant variation exists between the peak and residual friction angles before or after F-T cycling, which is consistent with Ladanyi and Theriault (1990). Besides, both the peak and residual interface friction angles at subzero temperatures are shown to be larger than the interface friction angle and the internal friction angle of the soil at thawed status. This behavior is not difficult to explain, as ice crystals not only enhance the interlock between soil particles but fill in the voids, contributing to the frictional resistance due to dilatancy. Yet the increase in both the peak and residual interface friction angles before F-T cycling is not significant, due to relatively low moisture content (≤ 20.8%) and degree of saturation (≤ 83.0%). Similar results can also be found in Aldaeef and Rayhani (2018) and Weaver and Morgenstern (1981).

Test results from Figs. 7 through 9 show that significant loss occurs between the peak and residual strengths of a frozen soil-concrete interface. It is believed that the strength loss mainly stems from the damage of ice bondage, or loss of ice adhesion, as the peak and residual friction angles do not vary significantly, before or after F-T cycling. This observation is consistent with the fact that large values of peak interface cohesion diminish to nearly zero in the residual state.

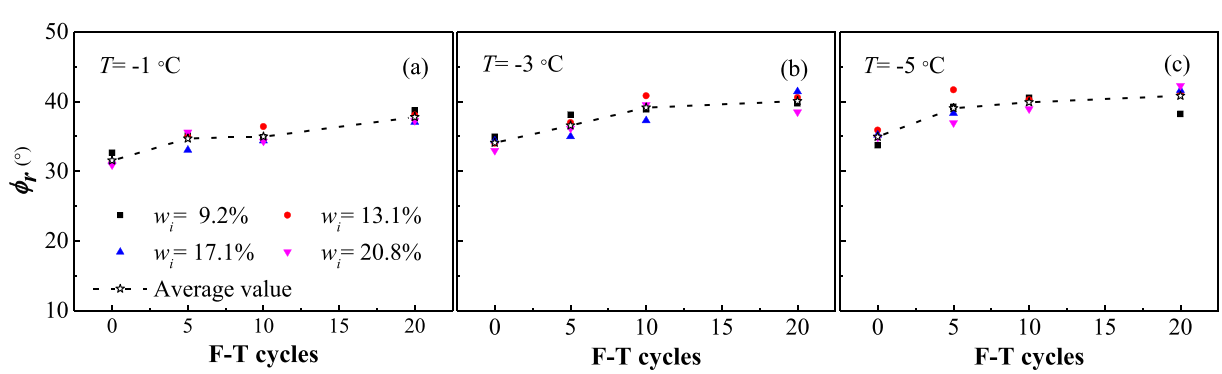

Fig. 18. Variation of the residual friction angle with F-T cycles at different temperatures and initial moisture contents.

4.2. Impact of F-T cycling

It was previously found that, during F-T cycling, the thermal flux through the soil-concrete interface induced by the higher thermal conductivity of concrete than soil helps drive the migration of unfrozen water from adjacent soil into the interface, resulting in the formation of an ice film at the frozen soil-concrete contact (e.g., Weaver and Morgenstern, 1981; Shoop and Bigl, 1997; Kim et al., 2003; Mu et al., 2010). Such ice films were also observed in specimens with higher initial moisture contents (i.e., 13.1%, 17.1%, and 20.8%) during this study and a previous study with similar soils (Wen et al., 2013). The moisture migration toward and formation of ice films at the interface was proved to have a significant influence on the mechanical behavior of a frozen soil-concrete interface (Sadovskiy, 1973; Ladanyi, 1995; Volokhov, 2003; Villeneuve, 2018; Weaver and Morgenstern, 1981). It is expected that the moisture content and degree of ice saturation in the frozen soil near the interface increases during F-T cycling, resulting in a significant increase in the peak and residual friction angles (6° to 9°) due to dilatancy and ice crystal interlock, as observed from this study.

The migration of moisture toward the interface can also help explain the gradual decrease in the dependence of peak displacement with the initial moisture content. As moisture migrates toward and accumulates at the interface after a large number of F-T cycling, say 20, it is the local moisture content of the soil adjacent to the interface that dominates the peak displacement, rendering the initial moisture content less significant, as vividly animated by Fig. 12.

Previous studies concluded that the shear strength of a frozen soil-concrete interface increases with increasing moisture content to a maximum and then decreases when the soil is supersaturated with ice (Sadovskiy, 1973; Ladanyi, 1995). For the specimens with a low initial moisture content such as 9.2%, the peak shear strength at −5 °C increases consistently with an increasing number of F-T cycling (refer to Fig. 14), due to moisture migration toward and accumulation of more ice crystals at the interface. For the specimens with higher initial moisture contents such as 13.1%, 17.1%, and 20.8%, however, moisture migration during continued F-T cycling can lead to oversaturation, formation, and gradual thickening of ice films at the interface at low temperatures, resulting in decreased interface shear strength, as observed in the same figure. Such a trend can also be noted on the peak cohesion at −5 °C in Fig. 15c, since it is one of the main components of the peak shear resistance.

5. Conclusions

This study investigated the shear behavior of a frozen soil-concrete interface by direct shear tests with an emphasis on F-T cycling impact. Sandy lean clay with different initial moisture contents (i.e., 9.2%, 13.1%, 17.1%, and 20.8%) and Portland cement concrete cylinders with its height precisely controlled were used to prepare specimens to ensure that the shear failure occurs at the soil-concrete interface. Specimens were conditioned at various sub-zero temperatures (i.e., −1 °C, −3 °C, and − 5 °C) and F-T cycles (i.e., 0, 5, 10, and 20) to obtain a series of test curves for analyses of the interface shear behavior. Experimental results including the shear stress-displacement curves, displacements and shear strengths at both peak and residual status, were presented and analyzed. Notably, the influence of F-T cycling on the interface behavior including peak and residual displacement and shear strength parameters were examined and discussed. The following conclusions can be drawn based on the results:

1) The peak displacement exhibits a linear relationship with the initial moisture content but is insensitive to temperature and normal stress.
2) The correlation between the peak displacement and the initial moisture content weakens as the number of F-T cycling increases. The peak displacement becomes almost independent of the initial moisture content after 20F-T cycles when it varies between 0.2 mm to 1.8 mm with a mean of 0.8 mm and a standard deviation of 0.4 mm.
3) The residual displacement is shown to be independent of the initial moisture content, temperature, normal stress, and F-T cycling and found to vary between 1 mm and 5 mm with a mean of 3.3 mm and a standard deviation of 1.0 mm.
4) Both the peak and residual friction angles of the frozen soil-concrete interface are larger than the interface friction angle or the internal friction angle of the soil at unfrozen status, especially after 10 to 20F-T cycling. While the residual friction angle is slightly larger than the peak one before F-T cycling, both gradually increase with an increasing number of F-T cycling. The maximum increase is 6° – 9° after 10 to 20F-T cycles.
5) The significant impact of F-T cycling on the interface shear behavior can be attributed to moisture migration toward, formation, and accumulation of ice films at the interface.

The findings from this study will help understand the behavior of a frozen soil-concrete interface, especially when F-T cycling is concerned. The shear strength parameters and the peak and residual displacements can be used to establish interface models for simulating the behavior of engineered geotechnical structures such as pile foundations, retaining walls, and earth dams or irrigation channels with concrete linings in the broad cold regions. Future study should consider more complex engineering conditions, such as uniaxial freezing, water supply, wet-dry cycling, etc.

Declaration of Competing Interest

As far as the authors know, there is no conflict of interests related to this manuscript.

Acknowledgments

The project was partially supported by the National Key Research and Development Program of China (No. 2017YFC0405101), the National Natural Science Foundation of China (No. 41772325 and No. 51878069), and the Teachers' Overseas Studies Program of Lanzhou University of Technology, Lanzhou, China.

References

Aldaeef, A.A., Rayhani, M.T., 2017. Adfreeze strength and creep behavior of pile foundations in warming permafrost. In: International Congress and Exhibition" Sustainable Civil Infrastructures: Innovative Infrastructure Geotechnology". Springer, Cham, pp. 254–264.
Aldaeef, A.A., Rayhani, M.T., 2018. Influence of exposure temperature on shaft capacity of steel piles in ice-poor and ice-rich frozen soils. In: International Congress and Exhibition "Sustainable Civil Infrastructures: Innovative Infrastructure Geotechnology". Springer, Cham, pp. 247–257.
Andersland, O.B., Alwahhab, M.R.M., 1982. Bond and slip of steel bars in frozen sand. In: CRREL Proc. of the 3d Intern. Symp. On Ground Freezing, pp. 27–34.
Biggar, K.W., Sego, D.C., 1993a. Field pile load tests in saline permafrost. i. Test procedures and results. Can. Geotech. J. 30 (1), 34–45.
Biggar, K.W., Sego, D.C., 1993b. Field pile load tests in saline permafrost. ii. Analysis of results. Can. Geotech. J. 30 (1), 46–59.
Bondarenko, G.I., Sadovskii, A.V., 1975. Strength and deformability of frozen soil in contact with rock. Soil Mech. Found. Eng. 12 (3), 174–178.
Choi, C., Lee, J., Kim, T.H., et al., 2014. Design Parameters of Micro Piles in Permafrost Sandy Ground. IWM, Krakow, Poland.
Feng, Q., Jiang, B.S., Zhang, Q., et al., 2016. Reliability research on the 5cm-thick insulation layer used in the Yuxi-Molegai tunnel based on a physical model test. Cold Reg. Sci. Technol. 124, 54–66.
Foriero, A., Ladanyi, B., 1995. FEM simulation of interface problem for laterally loaded piles in permafrost. Cold Reg. Sci. Technol. 23 (2), 121–136.
GBJ-82-85, 1997. The test method of long-term durability on ordinary concrete. In: National Standard of the People's Republic of China.
Gutierrez, M., Nygard, R., Hoeg, K., et al., 2008. Normalized undrained shear strength of clay shales. Eng. Geol. 99 (1–2), 31–39.
He, P.F., Ma, W., Mu, Y.H., et al., 2018. Study on freezing strength characteristics and formation mechanism of frozen soil-concrete interface. Trans. CSAE 34 (23), 127–133.
Hirayama, K., 1976. Thrust on hydraulic structures due to the thermal expansion of ice

cover. Technol. Rep. Iwate Univ. 9, 61–70.
Ji, Y.J., Hu, Y.P., Luo, T., 2019. The study of factors on the heat transfer characteristics of interface between cast-in-place concrete and frozen soil. In: IOP Conference Series: Earth and Environmental Science. 304 (5). IOP Publishing, pp. 052079.
Johnston, G.H., Ladanyi, B., 1972. Field tests of grouted rod anchors in permafrost. Can. Geotech. J. 9 (2), 176–194.
Kim, K.H., Jeon, S.E., Kim, J.K., et al., 2003. An experimental study on thermal conductivity of concrete. Cem. Concr. Res. 33 (3), 363–371.
Ladanyi, B., 1995. Frozen soil-structure interfaces. In: Selvadurai, A.P.S., Boulon, M.J. (Eds.), Mechanics of Geomaterial Interfaces. 42. pp. 3–33.
Ladanyi, B., Theriault, A., 1990. A study of some factors affecting the adfreeze bond of piles in permafrost. In: Proc. of Geotechnical Engineering Congress GSP 27 ASCE. vol. 1. pp. 213–224.
Lai, Y.M., Wu, Z., Liu, S., et al., 2002. Nonlinear analyses for coupled problem of temperature and seepage fields in cold regions retaining walls. J. Cold Reg. Eng. 16 (3), 156–167.
Li, G.Y., Ma, W., Zhao, S.P., et al., 2012. Effect of freeze-thaw cycles on mechanical behavior of compacted fine-grained soil. In: Morse, B., Dore, G. (Eds.), Cold Regions Engineering 2012: Sustainable Infrastructure Development in a Changing Cold Environment, Quebec City, Canada, pp. 72–81.
Li, G.Y., Wang, F., Ma, W., et al., 2018. Variations in strength and deformation of compacted loess exposed to wetting-drying and freeze-thaw cycles. Cold Reg. Sci. Technol. 151, 159–167.
Liu, H., Ling, H.I., 2008. Constitutive description of interface behavior including cyclic loading and particle breakage within the framework of critical state soil mechanics. Int. J. Numer. Anal. Met. 32 (12), 1495–1514.
Liu, J.K., Lv, P., Cui, Y., 2014a. Experimental study on direct shear behavior of frozen soil-concrete interface. Cold Reg. Sci. Technol. 104, 1–6.
Liu, J., Zou, D., Kong, X., 2014b. A three-dimensional state-dependent model of soil-structure interface for monotonic and cyclic loadings. Comput. Geotech. 61 (6), 166–177.
Liu, J.K., Chang, D., Yu, Q., 2016. Influence of freeze-thaw cycles on mechanical properties of a silty sand. Eng. Geol. 210, 23–32.
Lv, P., Liu, J.K., 2015. An experimental study on direct shear tests of frozen soil- concrete interface. J. Chin. Railw. Soc. 37 (2), 106–110.
Mu, R., Tian, W., Zhou, M., 2010. Moisture migration in concrete exposed to freeze-thaw cycles. J. Chin. Ceram. Soc. 38 (9), 1713–1717.
Neely, W.J., 2010. Collapse of MSE wall panels due to the effects of freezing temperatures. Earth Retent. Conf. 3, 580–587.
Nidowicz, B., Shur, Y.L., 1998. Russian and North American approaches to pile design in relation to frost action permafrost. In: Proceedings of the Seventh International Conference on Permafrost. Yellowknife, Canada.
Parameswaran, V.R., 1978. Adfreeze strength of frozen sand to model piles. Can. Geotech. J. 15 (4), 494–500.
Penner, E., Irwin, W.W., 1969. Adfreezing of Leda clay to anchored footing columns. Can. Geotech. J. 6 (3), 327–337.
Peretrukhin, N.A., Dubnov, Y.B., Merenkov, M.D., 1978. Study of the interaction of heaving ground with individual foundations. In: Proceedings 2nd International Conference on Permafrost. USSR Contribution, pp. 577–580.
Qi, J.L., Ma, W., Song, C., 2008. Influence of freeze-thaw on engineering properties of a silty soil. Cold Reg. Sci. Technol. 53, 397–404.
Qing, J., Tian, W., Lu, Y.C., et al., 2011. Experimental study on adhesion strength of freshwater ice frozen to concrete slab. Adv. Mater. Res. 243-249, 4587–4591.
Rui, D., Deng, H.Y., Nakamura, D., et al., 2016. Full-scale model test on prevention of frost heave of L-type retaining wall. Cold Reg. Sci. Technol. 132, 89–104.
Sadovskiy, A.V., 1973. Adfreeze between ground and foundation materials. In: 2nd Intl. Conf. On Permafrost, Yakutsk, North. Amer, pp. 650–653.
Sadzevicius, R., Damulevicius, V., Skominas, R., 2013. The technical state of earth dams in Lithuania. J. Environ. Eng. Landsc. Manag. 21 (3), 180–188.
Shen, Z.J., 2004. Weathering resistant design an important aspect of future development of geotechnical engineering design. Chin. J. Geotech. Eng. 26 (6), 866–869.
Shi, Q.B., Yang, P., Wang, G.L., 2018. Experimental research on adfreeze strengths at the interface between frozen fine sand and structures. Sci. Iran. 25 (2), 663–674.
Shoop, S.A., Bigl, S.R., 1997. Moisture migration during freeze and thaw of unsaturated soils: modeling and large-scale experiments. Cold Reg. Sci. Technol. 25 (1), 33–45.
Škerget, L., Tadeu, A., Brebbia, C.A., 2018. Transient simulation of coupled heat and moisture flow through a multi-layer porous solid exposed to solar heat flux. Int. J. Heat Mass Transf. 117, 273–279.
Sun, J.M., Li, G.Y., Zhang, Q.Y., et al., 1998. Stability analysis of earth-rock dam slope on the action of ice cover. J. Heilongjiang Hydraul. Eng. Coll. 1, 26–28 (in Chinese).
Tian, Y., Yang, Z.J., Tai, B., et al., 2019. Damage and mitigation of railway embankment drainage trench in warm permafrost: A case study. Eng. Geol. 261, 105276.
Viklander, P., 1998. Permeability and volume changes in till due to cyclic freeze/thaw. Can. Geotech. J. 35 (3), 471–477.
Viklander, P., Eigenbrod, D., 2000. Stone movements and permeability changes in till caused by freezing and thawing. Cold Reg. Sci. Technol. 31 (2), 151–162.
Villeneuve, J., 2018. Laboratory Testing for Adfreeze Bond of Sand on Model Steel Piles. University of Ottawa.
Volokhov, S.S., 2003. Effect of freezing conditions on the shear strength of soils frozen together with materials. Soil Mech. Found. Eng. 40 (6), 233–238.
Wang, T.L., Wang, H.H., Hu, T.F., et al., 2019. Experimental study on the mechanical properties of soil-structure interface under frozen conditions using an improved roughness algorithm. Cold Reg. Sci. Technol. 158, 62–68.
Weaver, J.S., Morgenstern, N.R., 1981. Simple shear creep tests on frozen soils. Can. Geotech. J. 18 (8), 217–229.
Wei, J.B., 2007. Analysis of harm of ice thrust to earth-filled dam and prevention measures. Sci. Technol. Innov. Herald. 10, 98 (in Chinese).
Wen, Z., Yu, Q., Ma, W., et al., 2013. Direct shear tests for mechanical characteristics of interface between Qinghai-Tibetan silt and fiberglass reinforced plastics. Rock Soil Mech. 34 (S2), 45–50.
Wen, Z., Yu, Q., Ma, W., et al., 2016. Experimental investigation on the effect of fiberglass reinforced plastic cover on adfreeze bond strength. Cold Reg. Sci. Technol. 131, 108–115.
Woo, S.K., Song, Y.C., Won, J.P., 2009. Durability of rock-filled-dam face-slab concrete. Proc. Inst. Civ. Eng. 162 (2), 73–79.
Wu, G., Bing, H., Bu, D.S., 2019. Experimental study on the relationship between saline soil and salt solution freezing temperature. J. Glaciol. Geocryol. 41 (3).
Zhang, Z., Ma, W., Feng, W.J., et al., 2016. Reconstruction of soil particle composition during freeze-thaw cycling: a review. Pedosphere 26 (2), 167–179.
Zhao, L.J., Yang, P., Wang, J.G., et al., 2014. Impacts of surface roughness and loading conditions on cyclic direct shear behaviors of an artificial frozen silt–structure interface. Cold Reg. Sci. Technol. 106, 183–193.
Zhu, M., Michalowski, R.L., 2013. A numerical approach to simulate soil freezing and frost heave behind an earth retaining structure. J. Comput. Civ. Eng. 2013, 307–314.